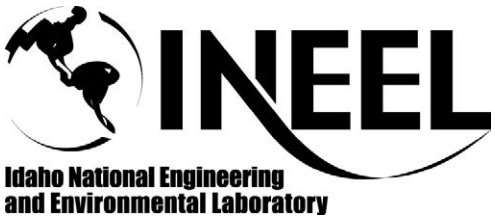

Idaho National Engineering
and Environmental Laboratory

INEEL/CON-02-01383
PREPRINT

Extensions To SCDAP/RELAP5-3D For Analysis Of Advanced Reactors

E. A. Harvego
L. J. Siefken

April 20, 2003

11th International Conference On Nuclear Engineering

This is a preprint of a paper intended for publication in a journal or proceedings. Since changes may be made before publication, this preprint should not be cited or reproduced without permission of the author.
This document was prepared as a account of work sponsored by an agency of the United States Government. Neither the United States Government nor any agency thereof, or any of their employees, makes any warranty, expressed or implied, or assumes any legal liability or responsibility for any third party's use, or the results of such use, of any information, apparatus, product or process disclosed in this report, or represents that its use by such third party would not infringe privately owned rights. The views expressed in this paper are not necessarily those of the U.S. Government or the sponsoring agency.

11th International Conference on Nuclear Engineering
Tokyo, JAPAN, April 20-23, 2003
ICONE11-36420

EXTENSIONS TO SCDAP/RELAP5-3D FOR ANALYSIS OF ADVANCED REACTORS

E. A. Harvego
Idaho National Engineering and Environmental Laboratory
P.O.Box 1625
Idaho Falls, Idaho 83415
Phone: (208) 526-9544
Fax: (208) 526-2930
e-mail: hae@inel.gov

L. J. Siefken
Idaho National Engineering and Environmental Laboratory
P.O.Box 1625
Idaho Falls, Idaho 83415
Phone: (208) 526-9319
Fax: (208) 526-2930
e-mail: ljs@inel.gov

Keywords: SCDAP/RELAP5-3D, advanced reactor modeling, HTGR, advanced fuel design.

ABSTRACT

The SCDAP/RELAP5-3D code was extended to enable the code to perform transient analyses of advanced LWRs (Light Water Reactors) and HTGRs (High Temperature Gas Reactors). The extensions for LWRs included: (1) representation of micro-heterogeneous fuel varying in composition in the radial and axial directions, (2) modeling of two-dimensional radial/axial heat conduction for more accurate calculation of fuel and cladding temperatures during the reflood period of a large break loss-of-coolant accident (LOCA), (3) modeling of fuel-cladding interface pressure and fuel-cladding gap conductance, (4) representation of radial power profiles varying in a discontinuous manner in the axial direction, and (5) addition of material properties for fuel composed of mixtures of ThO_2-UO_2 and ThO_2-PuO_2. The extensions for HTGR analyses included: (1) modeling of the transient two-dimensional temperature behavior of graphite moderated reactor cores (pebble bed and block-type), reactor vessel, and reactor containment, (2) modeling of flow losses and convective heat transfer in pebble bed reactor cores, (3) modeling of oxidation of graphite components in reactor cores due to the ingress of air and/or water, and (4) modeling of the affect of oxidation on the composition of gases in the reactor system. The applications of the extended code to LWR analyses showed that advanced fuels intended for proliferation resistance and waste reduction could also be designed to produce calculated peak cladding temperatures during a large break LOCA less than the 1477 K acceptance criterion in 10 CFR 50.46. Fuels composed of ThO_2-UO_2 and ThO_2-PuO_2 are examples of such fuels. The applications of the extended code to HTGR analyses showed that: (1) HTGRs can be designed for passive removal of all decay heat, and (2)

Copyright © 2003 by JSME

fuel damage from air ingress accidents may be reduced or prevented by the consumption of ingressing oxygen by reflector material located below the core.

1. INTRODUCTION

The importance of nuclear energy as a vital and strategic resource in the U.S. and world's energy mix has led to an initiative termed Generation IV by the U.S. Department of Energy (DOE), to develop and demonstrate new and improved reactor technologies. These new Generation IV reactor concepts are expected to be substantially improved over the current generation of reactors with respect to economics, safety, proliferation resistance and waste characteristics. However, adequate assessment of the performance of these advanced reactor concepts requires extensions to existing state-of-the-art analysis tools developed for the detailed analysis of commercial light water reactors. In particular, the focus of this paper is on the extensions to the INEEL-developed SCDAP/RELAP5-3D and its application to advance light water reactor concepts utilizing advanced fuel designs for proliferation resistance and waste reduction, and gas-cooled reactors with inherently safe design features.

Section 2 of this paper provides a brief description of the INEEL-developed SCDAP/RELAP5-3D code, and its current capabilities with respect to the analysis of current generation reactors. This is followed in Section 3 with a description of modeling improvements made to the code for analysis of advanced light water reactor fuels with improved proliferation resistance and waste reduction characteristics. Included in Section 3 are results of SCDAP/RELAP5-3D analyses demonstrating the modeling capabilities of the code and the performance characteristics of advanced light water reactor fuels with respect to current safety requirements. Section 4 of this paper describes extensions made to the SCDAP/RELAP5-3D code for analyses of advanced gas-cooled reactor concepts, and includes results of calculations performed to demonstrate the functionality of these extensions in predicting the behavior of gas-cooled reactors subjected to extreme accident conditions. Finally, Section 5 of this paper presents conclusions from the development work performed to date on the SCDAP/RELAP5-3D code, and summarizes future plans for continued development of the code in support of the DOE Generation IV initiative.

2. DESCRIPTION OF SCDAP/RELAP5-3D

The SCDAP/RELAP5-3D code (Siefken et. al., 2001, SCDAP/RELAP5-3D Code Development Team, 2002) is an extension of the RELAP5-3D computer code (RELAP5-3D 1999), that has been developed primarily for the thermal-hydraulic analyses of light water nuclear reactors and related experimental systems. The RELAP5-3D code can simulate a wide variety of thermal-hydraulic transients involving steam, water, and non-condensable fluid mixtures. These transients include design-basis loss-of-coolant accidents and operational events in commercial pressurized and boiling water reactors, test and production reactors operated by the DOE, and related experimental systems.

The components of a nuclear reactor are represented with a user-defined nodalization that contains hydrodynamic control volumes and heat structures. The code solves separate continuity, momentum, and energy equations for the gas and liquid phases. Within each control volume, each phase can have a different temperature and velocity. The code contains heat conduction and wall heat transfer models to simulate the energy exchange between structures and hydrodynamic control volumes. The code contains models to represent the nuclear kinetics of a reactor core. The code also contains a flexible control system that allows the user to represent physical control systems within plants.

The predecessor RELAP5 code (RELAP5 1995) was originally developed for one-dimensional applications and utilized one-dimensional hydrodynamic and heat conduction models and a point reactor kinetics model, in which the spatial distribution of power generated by the reactor remained fixed. The RELAP5-3D code has been improved and contains multi-dimensional hydrodynamic and reactor kinetics models.

The SCDAP/RELAP5-3D code (SCDAP/RELAP5-3D Code Development Team, 2002) has been developed to allow calculation of light water nuclear reactor system response for beyond-design-basis accidents, including core damage. The code is the result of merging RELAP5-3D with the SCDAP models for predicting fuel rod behavior and core degradation characteristics under extreme or limiting accident conditions.

Reactor systems can be modeled using an arbitrary number of fluid control volumes and connecting junctions, core components and system components. Flow areas, volumes, and flow resistances can vary with time through either user-control or models that describe the changes in geometry associated with damage in the core. Transient temperature distributions in structures can be modeled with RELAP5 one-dimensional heat structures, SCDAP two-dimensional heat structures, or SCDAP two-dimensional porous medium heat structures. The SCDAP heat structures include heat structures designed to specifically represent light water reactor fuel rods, silver-indium-cadmium (Ag-In-Cd) and B_4C

Copyright © 2003 by JSME

control rods and/or blades, electrically heated fuel rod simulators, and structures such as reactor vessels and concrete structures. Other system components available to the user include pumps, valves, electric heaters, jet pumps, turbines, separators and accumulators.

The code is particularly well suited for analysis of a variety of advanced fuel designs because the steady-state and transient modeling of the structural, thermal, and chemical behavior of fuels is readily extended to different fuel forms and geometries, and the detailed mechanistic fuel models are comparable to those in current standalone state-of-the-art fuel codes such as FRAPCON-3 (Berna et al 1997) and FRAP-T6 (Siefken et al 1981). In addition, the ability to model a variety of reactor coolants (water, gas, and liquid metal) provides a unique integrated analysis capability not available in other detailed analysis codes.

3. MODELING OF ADVANCED LWR FUELS

ThO_2-UO_2 fuel designs are being considered for applications in advanced light water reactors because of their potential improved economics, as well as their proliferation resistance, safety, and long-term disposal characteristics. Over the last three years, a collaborative research program that included the INEEL, Massachusetts Institute of Technology (MIT), Framatome, and the Korean Atomic Energy Research Institute has been conducted to characterize the performance of ThO_2-UO_2 fuels (MacDonald 2002). The research included the evaluation of ThO_2-UO_2 neutronic characteristics, steady state and transient fuel behavior, fabrication costs, and long-term disposition in a geological depository. INEEL's role in this effort, which is the focus of this section of the paper, was the calculation of the transient behavior of a wide range of ThO_2-UO_2 designs for use in advanced or current generation reactors. The performance of these calculations required a number of extensions to the SCDAP/RELAP5-3D and FRAPCON-3 codes. These extensions included (1) the capability to represent fuel composition varying in both the radial and axial directions, (2) development of a moving fine-mesh for calculation of 2-D axial and radial heat conduction during the reflood period of a loss-of-coolant accident (LOCA), (3) development of models for calculating fuel-cladding interface pressure and gap conductance at relatively high temperature and burnup conditions, (4) representation of the radial power profile varying with elevation, and (5) linking of SCDAP/RELAP5-3D to the FRAPCON-3 steady-state fuel analysis code.

A detailed description of the above models and their implementation into the SCDAP/RELAP5-3D code is contained in MacDonald and Herring 2001 through MacDonald 2002. The development of improved models for calculating fuel-cladding interface pressure and gap conductance (Item 3 above) was required because the high temperatures and burnup of the ThO_2-UO_2 driver fuel leads to relatively firm contact between the fuel and cladding, and associated higher fuel-cladding interface pressures and gap conductance. The modeling of radial power profiles within the fuel varying with elevation (Item 4) was necessary because, while beginning-of-life fuel rods have a power density that is almost uniform from the centerline to the surface of the pellet, fuel rods with a high burnup can have power densities near the pellet surface that are double the average power density of the fuel rod. Finally, the linking of SCDAP/RELAP5-3D with FRAPCON-3 (Item 5) allows transient calculations to be initialized with burnup-dependent fuel conditions, including fission gas release, fuel swelling, cladding creep-down, and changes in radial power profile.

The best neutronics and long-term burnup of ThO_2-UO_2 was achieved with an axially and radially micro-heterogeneous fuel composition design. The fuel design, shown in Figure 1, involved an alternate stacking of driver and blanket sections of fuel, with the driver sections having a graphite core surrounded by an annulus of enriched UO_2, and the blanket (seed) section having a core of enriched UO_2 surrounded by an annulus of 100% ThO_2. Each driver section was 40 mm in height and each seed section was 91.6 mm in height, giving a total of 28 driver-seed pairs in a typical 3.66-m long fuel rod. As burnup occurs in the fuel, fissile U_{233} is created in the ThO_2. As burnup proceeds, the heat generation shifts from being primarily in the driver sections to being about equally distributed between the driver and seed sections.

At the beginning of life, Figure 2 shows that the power production in the ThO_2-UO_2 fuel is much greater in the driver section than in the seed section. Although the driver section length is only half that of the seed section, nevertheless, the driver section produces more than twice the power of the seed section. The peak linear power in the driver section occurs near the interface of the driver and the blanket sections. At the core mid-plane, where the axial peak in power occurs, the axially averaged linear power in the driver section is 81 kW/m and the axially averaged linear power in the adjacent seed section is only 25 kW/m.

A SCDAP/RELAP5-3D calculation of the beginning-of-life steady-state temperature distribution for this fuel configuration is shown in Figure 3. This calculation was performed for the highest power driver and seed sections by modeling the two-dimensional radial/axial temperature distribution with a fine axial

Copyright © 2003 by JSME

mesh overlaying the pair of driver-seed sections. The axially averaged linear power in this pair of driver-seed sections was 42.2 kW/m. The axial nodes were spaced 1 mm apart in this pair of driver-seed sections, which is a spacing of the same order of magnitude as that used for the radial nodes. Figure 3 plots as a function of elevation the temperature at the fuel centerline and at a radius of 1.72 mm, beginning at the mid-plane of the driver section and ending at the mid-plane of the seed section. As shown in the plot, the maximum steady-state fuel temperature of 2750 K does not occur in the driver section, where the linear power is the greatest, but instead occurs at the mid-plane of the seed section. This behavior occurs because the heat generation in the driver section is located in the outer portion of the fuel, where there is a relatively short distance for conducting heat to the cladding, while the heat generation in the seed section occurs in the central region of the fuel, where there is a longer conduction path to the cladding. The differences in conduction heat removal characteristics between the driver and seed sections are also apparent in the radial temperature distributions shown in Figure 3. Since the heat generation in the driver section is all outside the 1.72-mm radius, there is a flat temperature profile (no radial temperature difference) between the centerline and 1.72-mm radius of the driver section. In contrast, the radial temperature difference between the centerline and 1.72-mm radius of the seed section is relatively large because heat generated by the UO_2 in the center of the seed section is conducted radially outward through the ThO_2 annulus to the fuel cladding.

To determine the impact of the above beginning-of-life power and temperature characteristics for this micro-heterogeneous ThO_2-UO_2 fuel design, a SCDAP/RELAP5-3D calculation of a large-break loss-of-coolant accident (LOCA) was performed using an existing SCDAP/RELAP5-3D model of the Seabrook pressurized water reactor (PWR) (Jones et al 1992). Three flow channels represented the fluid space in the core region, each with a stack of nine control volumes connected to each other with cross-flow junctions. In the hot bundle location of the reactor core, both ThO_2-UO_2 and 100% UO_2 (typical of commercial) fuel rods were modeled. The peak average linear power in these fuel rods was 42.2kW/m. For the pair of driver-seed sections in the ThO_2-UO_2 fuel rod at the elevation of peak power, the axially averaged linear powers in the driver and seed sections were 81 kW/m and 25 kW/m, respectively. To model the axial heat conduction in the fuel, the driver-seed pair at the peak axial power location was modeled with 66 axial nodes spaced 1 mm apart, and the balance of the rod was modeled with eight axial nodes. The results of the LOCA calculation are shown in Figure 4, which compares the transient cladding temperatures during the LOCA of the ThO_2-UO_2 and UO_2 fuel rods at the mid-plane elevation. The somewhat higher initial stored energy in the ThO_2-UO_2 fuel (DuAx4 fuel) at the start of the LOCA compared with that in the 100% UO_2 fuel resulted in about a 150 K higher maximum cladding temperature for the ThO_2-UO_2 fuel, but the maximum cladding temperature for both fuels was still less than the 1477 K Nuclear Regulatory Commission (NRC) acceptance criteria.

4. MODELING OF GAS-COOLED REACTORS

High-temperature gas-cooled reactors (HTGRs) are strong candidates for Generation IV consideration because of their relatively high power conversion efficiencies and benign behavior under accident conditions. This benign behavior is derived from the inherent characteristics of the inert helium coolant, a low reactor core power density, coated fuel particles for fission product retention, a high thermal capacity graphite matrix core design, and specific design features to ensure passive safety.

Two basic HTGR designs have been developed. The first type, namely the pebble-bed core, has the fuel embedded within graphite pebbles through which the helium coolant is forced. Each graphite fuel pebble, which is about 50 mm in diameter, contains many small, coated fuel particles. Pebbles composed only of graphite are also included with the matrix of fuel pebbles to moderate the neutrons produced by the fission of the fuel. An annulus of graphite blocks is also placed around the reactor core to moderate the neutrons. The pebble-bed HTGR is also designed for continuous on-load refueling in which the pebbles are fed into the top of the operating reactor and then move downward by gravity. After about three months of irradiation, the individual fuel pebbles exit from the bottom of the reactor at a rate of about two pebbles per minute. Graphite pebbles are also fed into the center of the top of the reactor core and then move downward in parallel with the fuel pebbles. Each fuel pebble passes through the reactor about ten times and will be in the reactor for a total of about three years.

The second type of core design, namely the block-type or prismatic core design has the fuel configured as rods (compacts) inside blocks of graphite. Each fuel rod contains many small, coated fuel particles. The helium in this case, flows downward through vertical coolant holes in the graphite blocks.

Since SCDAP/RELAP5-3D is a generalized system thermal-hydraulic code with the capability to include different coolant and material properties, including

Copyright © 2003 by JSME

helium coolant and graphite fuel and core structures, the fundamental requirements for modeling the thermal-hydraulic behavior of gas-cooled reactors already existed. However, two hypothetical gas-cooled reactor transients could not be modeled directly without modeling extensions. These two transients were an air or water ingress accident due to a pipe break, and a conduction cool-down accident involving a complete loss of helium coolant requiring heat removal by radial conduction and radiation from the reactor core, through the reflector and reactor vessel structures to the reactor cavity cooling system or ultimate earth heat sink. In addition, the unique design of the Pebble Bed HTGR core required extensions to code models for calculating heat transfer and flow losses through the bed of graphite pebbles.

The modeling of a conduction cool-down accident basically involved the development of separate SCDAP heat structures for the pebble-bed and prismatic or block-type reactor core designs that account for radial heat transfer by conduction and radiation from the reactor core to the ultimate earth heat sink. While the calculation of a conduction cool-down accident could be performed in an approximate manner with previously existing input options in SCDAP/RELAP5-3D, the development of specific user-defined SCDAP heat structures for HTGRs significantly simplifies the input requirements. A representation of the model used for calculating heat removal by conduction and radiation through the various reactor core and structure components to the ultimate earth heat sink is shown in Figure 5.

The modeling of graphite oxidation caused by either air or water ingress is documented in Siefken 2002. The oxidation models for both air and water ingress require the capability to define a fine axial mesh in the regions in which oxidation occurs. A fine axial nodalization is required because a possibly small bulk flow rate of air or water limits the oxidation to a relatively small region. The location of this small region is dependent upon the temperature distribution in the reactor core at the time of the air or water ingress and cannot be determined a priori.

Figure 6 shows a SCDAP/RELAP5-3D calculation of the heat up of a pebble-bed HTGR during a conduction cool-down accident with air ingress. The calculation was performed with a simplified model of a representative conceptual design for a pebble-bed HTGR. A reactor power of 265 MW thermal was assumed. The fuel part of the reactor core is 8.5-m high. The core has graphite reflectors at its side, bottom and top. The fueled part of the core has a diameter of 3.5 m.

The reactor core was modeled with 90 axial nodes and 19 radial nodes, and the reactor vessel was modeled with 90 axial nodes and 5 radial nodes. The containment and earth were modeled with 90 axial nodes and 21 radial nodes. The fluid in the core was modeled with a stack of 90 RELAP5 control volumes.

For this analysis, the blowdown phase of the accident was not modeled and the only heat generation in the reactor core was assumed to be that due to decay heat. The heat up phase of the accident (start of conduction cool-down) was assumed to begin with the reactor core and vessel at a temperature of 600 K and the reactor containment and the earth at an initial temperature of 300 K. At 72,000 s after the start of the accident (20 hours), air was assumed to ingress into the reactor core at a velocity of 0.066 m/s.

Plotted in Figure 6 are the maximum core temperature, maximum reactor vessel temperature, and the maximum containment wall temperature during the conduction cool-down. At 72,000 s after the start of the heat up phase, the maximum core temperature was calculated to be about 1250 K. At this time (as indicated in Figure 6) air ingress into the bottom of the reactor vessel was initiated. However, this air ingress had no affect on the maximum core temperature, which continued to slowly increase in temperature due to the core decay heat.

The reason that air ingress did not influence the maximum core temperature is because all of the ingressed air was consumed by the oxidation of graphite in the lower and cooler core region. This is shown in Figure 7, which plots the temperature response of the reactor core at the 0.54-m and 0.06-m elevations for an air ingress rate of 0.066 m/s. Also plotted in this figure is the temperature response of the reactor core at the 0.06-m elevation for an air ingress rate of 0.033 m/s. This figure shows that the temperature response of the bottom of the core (0.06-m elevation) was strongly dependent on the air ingress rate, indicating that the rate of graphite oxidation in this area was determined by the bulk flow rate of air supplying the oxygen for the reaction process. Also, since the temperature response of the fuel rods at the 0.54-m elevation was hardly affected by the air ingress rate, little oxidation of graphite occurred at the higher elevations of the core. In fact, essentially all the oxygen in the air was consumed by the graphite in the lower 0.2-m of the core, and thus no oxygen was available for oxidation of the graphite in the higher elevations of the reactor core. core, and thus no oxygen was available for oxidation of the graphite in the higher elevations of the reactor core.

5. CONCLUSIONS

Significant modeling improvements and extensions have been incorporated into the SCDAP/RELAP5-3D

Copyright © 2003 by JSME

code that enables the code to perform transient analyses for a wide range of Generation IV reactors. The focus of this paper is on improvements made to the code for the analysis of advanced LWR fuels with improved proliferation resistance and reduced waste characteristics, and on code modeling of gas-cooled reactor transient behavior.

Improvements made for the modeling of advanced LWR fuels include: (1) representation of micro-heterogeneous fuel varying in composition in the radial and axial directions, (2) modeling of two-dimensional radial/axial heat conduction for more accurate calculation of fuel and cladding temperatures during the reflood period of a LOCA, (3) modeling of fuel-cladding interface pressure and fuel-cladding gap conductance, (4) representation of radial power profiles varying in a discontinuous manner in the axial direction, and (5) addition of material properties for fuel composed of mixtures of ThO_2-UO_2 and ThO_2-PuO_2.

The extensions for HTGR analyses included: (1) modeling of the transient two-dimensional temperature behavior of graphite moderated reactor cores (pebble bed and block-type), reactor vessel, and reactor containment, (2) modeling of flow losses and convective heat transfer in pebble bed reactor cores, (3) modeling of oxidation of graphite components in reactor cores due to the ingress of air and/or water, and (4) modeling of affect of oxidation on composition of gases in the reactor system.

The applications of the extended code to LWR analyses showed that advanced fuels intended for proliferation resistance and waste reduction could also be designed to produce calculated peak cladding temperatures during a large break LOCA less than the 1477 K acceptance criterion in 10 CFR 50.46. Fuels composed of ThO_2-UO_2 and ThO_2-PuO_2 are examples of such fuels. The applications of the extended code to HTGR analyses showed that: (1) HTGRs can be designed for passive removal of all decay heat, and (2) fuel damage from air ingress accidents may be reduced or prevented by the consumption of ingressing oxygen by reflector material located below the core.

REFERENCES

Berna, G. A., C. E. Beyer, K. L. Davis, and D. D. Lanning, FRAPCON-3: A Computer Code for the Calculation of Steady-State Thermal-Mechanical Behavior of Oxide Fuel Rods for High Burnup, PNNL-11513, NUREG/CR-6534, 1997.

Jones, K. R., N. L. Wade, K. R. Katsma, L. J. Siefken, and M. Straka, Timing Analysis of PWR Fuel Pin Failures, NUREG/CR-5787, EGG-2657, Vol. 1, September 1992.

MacDonald, P. E., and J. S. Herring, Advanced Proliferation Resistant, Lower Cost, Uranium-Thorium Dioxide Fuels for Light Water Reactors, NERI Project 99-0153, Progress Report for Work through August, 2001, 1st Annual Report, Idaho National Engineering and Environmental Laboratory, Idaho Falls, ID, INEL/EXT-2000-01217.

MacDonald, P. E., Advanced Proliferation Resistant, Lower Cost, Uranium-Thorium Dioxide Fuels for Light Water Reactors, NERI Project 99-0153, Progress Report for Work through November 2000, Idaho National Engineering and Environmental Laboratory, Idaho Falls, ID, INEL/EXT-2001-01656, January 2001.

MacDonald, P. E., Advanced Proliferation Resistant, Lower Cost, Uranium-Thorium Dioxide Fuels for Light Water Reactors, NERI Project 99-0153, Progress Report for Work through May 2001, Idaho National Engineering and Environmental Laboratory, Idaho Falls, ID, INEL/EXT-01-00804, June 2001.

MacDonald, P. E., Advanced Proliferation Resistant, Lower Cost, Uranium-Thorium Dioxide Fuels for Light Water Reactors, NERI Project 99-0153, Progress Report for Work through August, 2001, 2nd Annual Report, Idaho National Engineering and Environmental Laboratory, Idaho Falls, ID, INEL/EXT-01-00804.

MacDonald, P. E., Advanced Proliferation Resistant, Lower Cost, Uranium-Thorium Dioxide Fuels for Light Water Reactors, NERI Project 99-0153, Progress Report for Work through November 2001, Idaho National Engineering and Environmental Laboratory, Idaho Falls, ID, INEL/EXT-02-00308, 2002.

MacDonald, P. E., Advanced Proliferation Resistant, Lower Cost, Uranium-Thorium Dioxide Fuels for Light Water Reactors, NERI Project 99-0153, Progress Report for Work through May 2002, Idaho National Engineering and Environmental Laboratory, Idaho Falls, ID, INEL/EXT-02-00924.

The RELAP5 Development Team, RELAP5/MOD3 Code Manual, Vol. IV: Models and Correlations, NUREG/CR-5535, INEL-95/0174, August 1995.

The RELAP5-3D Development Team, RELAP5-3D Code Manual, Volume 1: Code Structure, System Models and Solution Methods, INEEL-EXT-98-00834, Revision 1.1b, 1999.

SCDAP/RELAP5-3D Code Development Team, SCDAP/RELAP5-3D Code Manual, INEEL/EXT-02-00589, 2002.

Siefken, L. J., C. M. Allison, M. P. Bohn, and S. O. Peck, FRAP-T6: A Computer Code for the Transient Analysis of Oxide Fuel Rods, NUREG/CR-2148, EGG-2104, May 1981.

Siefken, L. J., E. W. Coryell, E. A. Harvego, and J. K. Hohorst, SCDAP/RELAP5/MOD3.3 Code Manual:

Copyright © 2003 by JSME

Modeling of Reactor Core and Vessel Behavior During Severe Accidents, NUREG/CR-6150, Vol. 2, Rev. 2, INEL-96/0422, January 2001.

Siefken, L. J., E. W. Coryell, and E. A. Harvego, Conceptual Designs of Models for the Transient Analysis of Pebble Bed temperature Reactors, INEEL/INT-02-00154, January 2002.

Copyright © 2003 by JSME

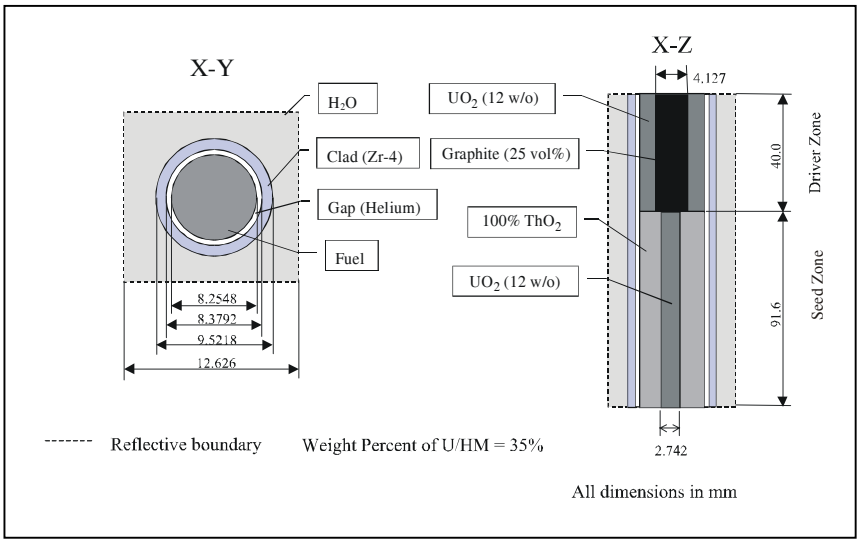

Figure 1. Design of ThO_2-UO_2 fuel with capability for high burnup.

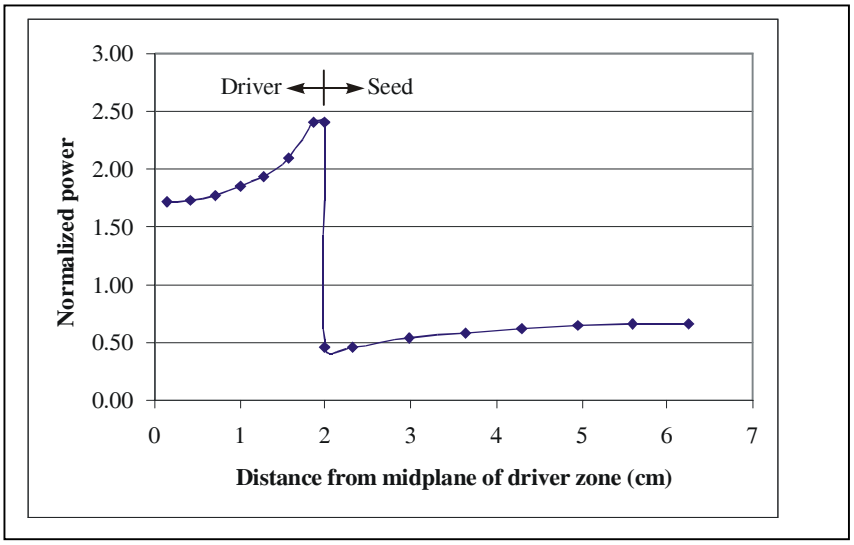

Figure 2. Axial power distribution in heterogeneous fuel.

Copyright © 2003 by JSME

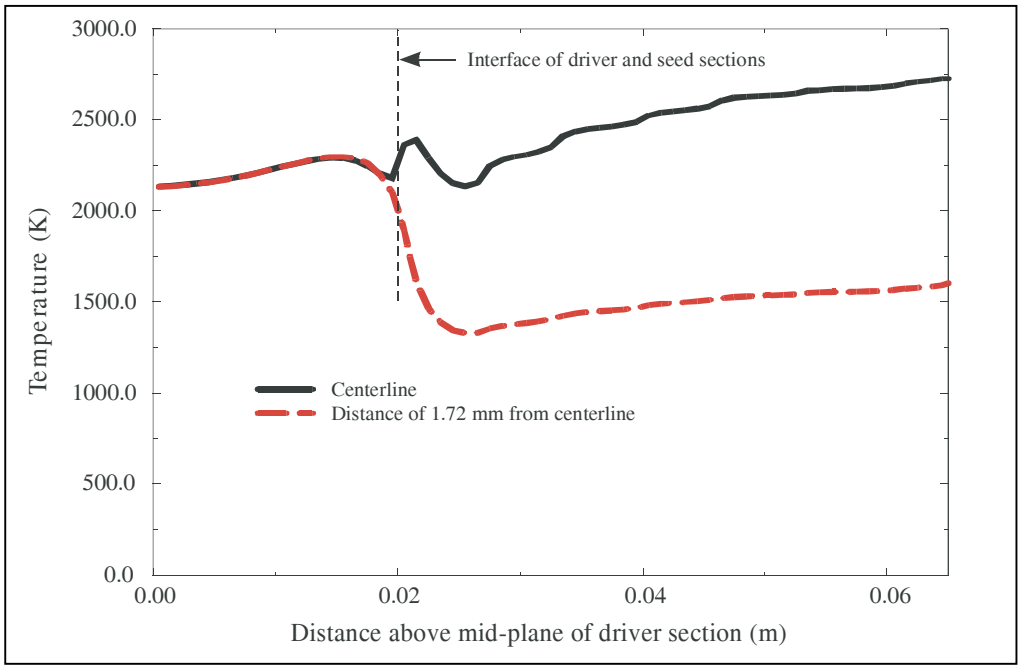

Figure 3. Steady-state temperature distribution in heterogeneous fuel.

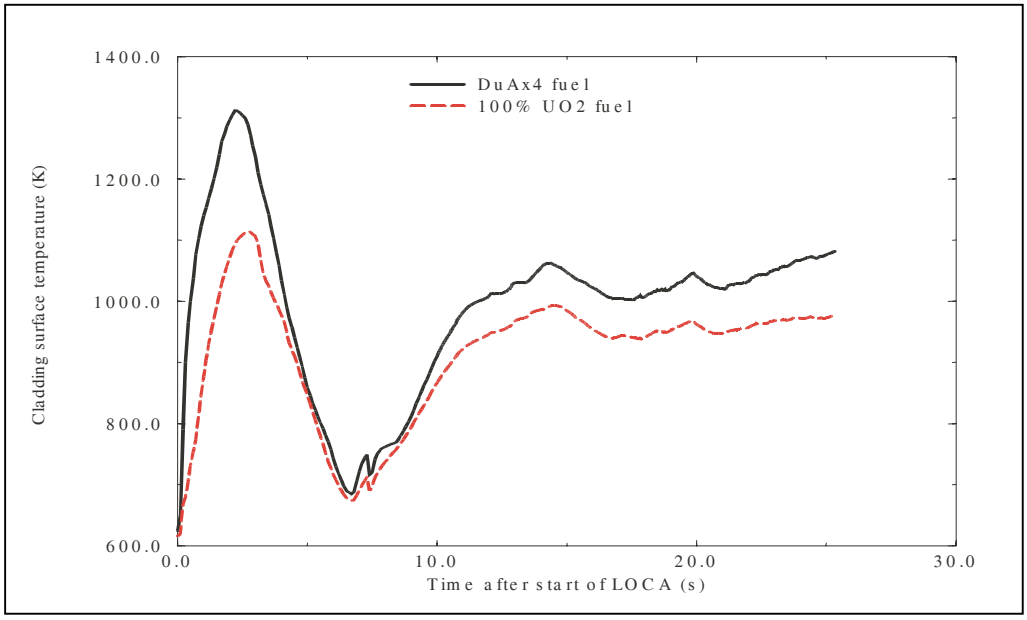

Figure 4. Maximum cladding temperature of heterogeneous fuel during large break LOCA.

Copyright © 2003 by JSME

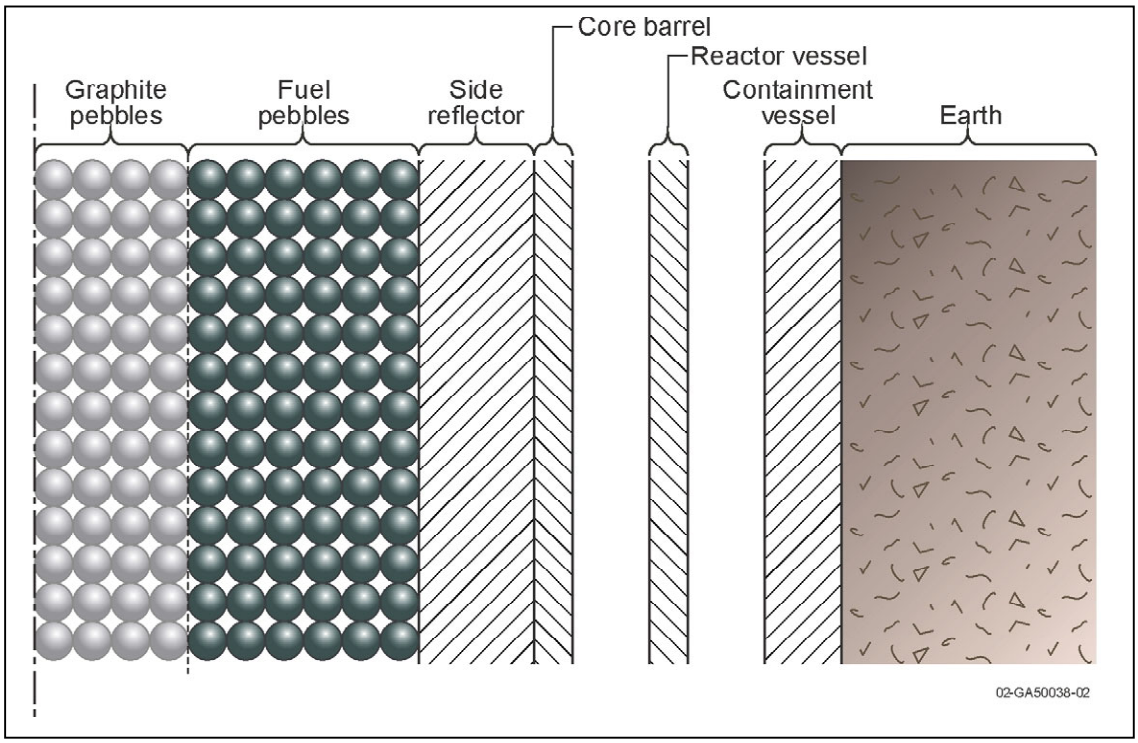

Figure 5. Representation of model for conduction cooldown of a pebble-bed HTGR.

Copyright © 2003 by JSME

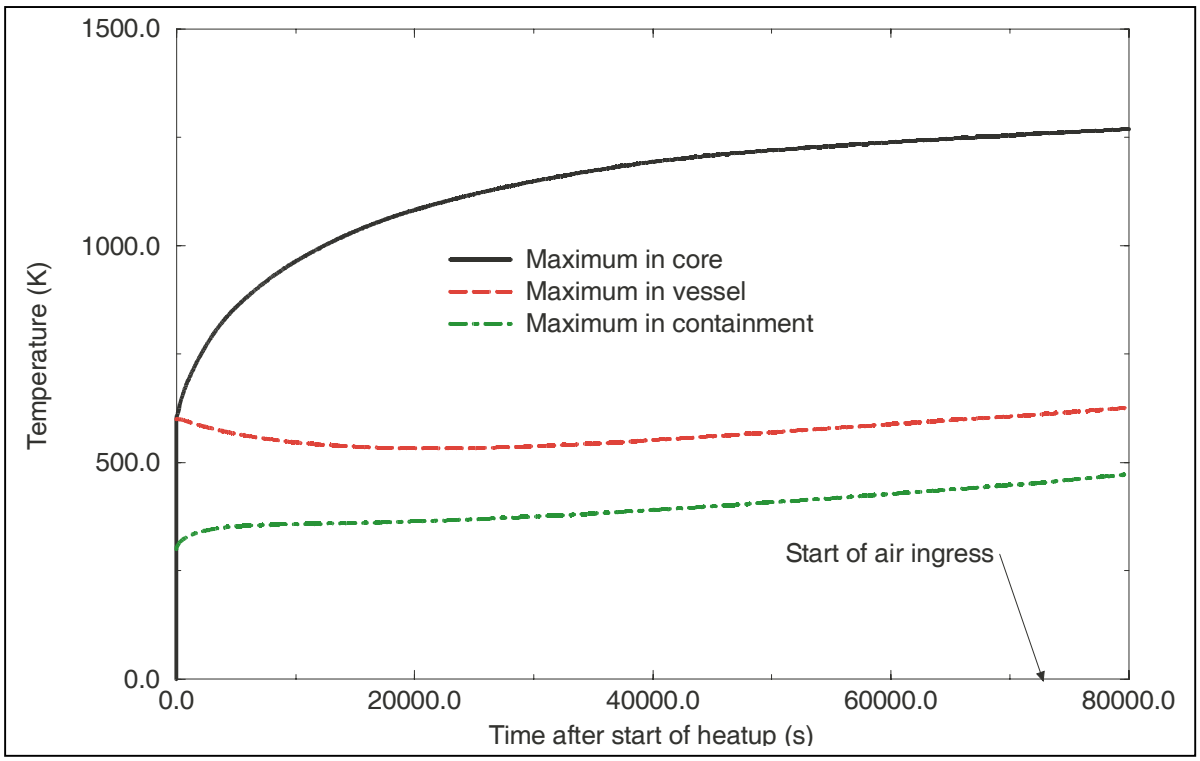

Figure 6. Long-term temperature distribution in reactor core, vessel and containment for generic HTGR.

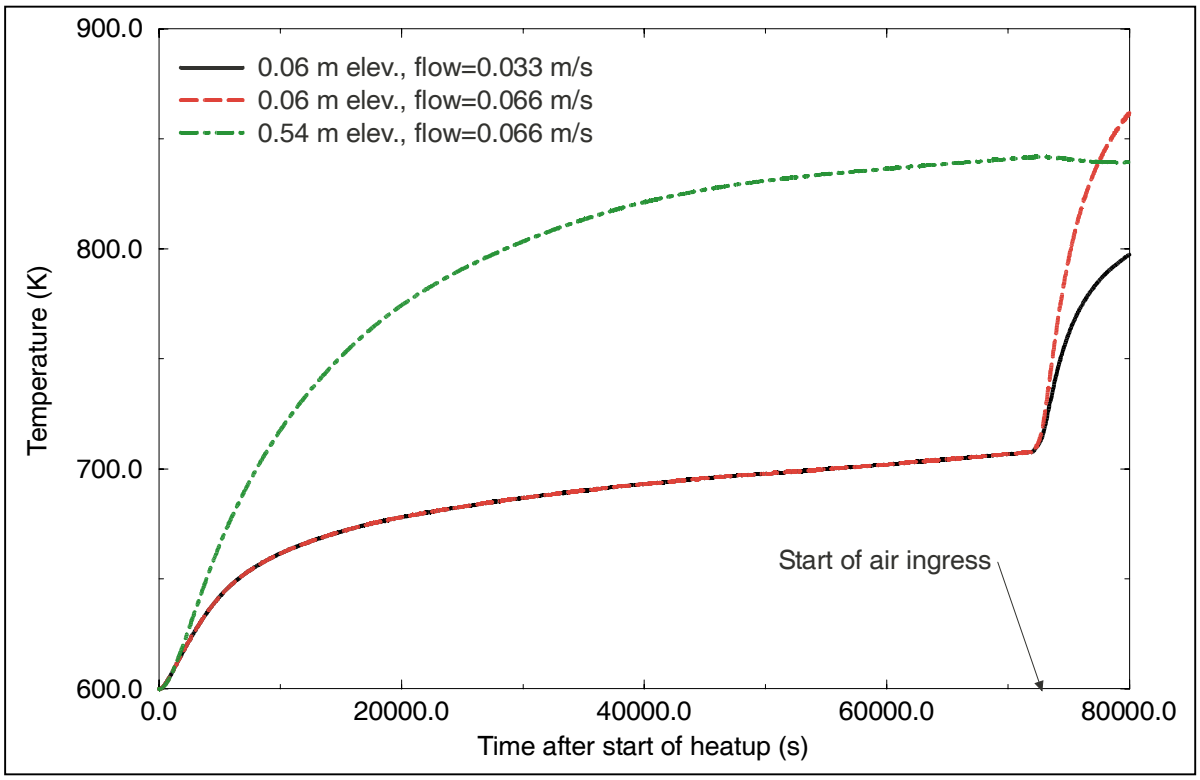

Figure 7. Core temperature response caused by oxidation of graphite.

Copyright © 2003 by JSME